

Using computational fluid dynamics in combating erosion–corrosion

Srdjan Nešić*

The Department of Mechanical Engineering, University of Queensland, Brisbane, Qld 4000, Australia

Received 14 January 2005; received in revised form 29 December 2005; accepted 30 January 2006

Available online 22 March 2006

Abstract

Computational fluid dynamics was used to search for the links between the observed pattern of attack seen in a bauxite refinery's heat exchanger headers and the hydrodynamics inside the header. Validation of the computational fluid dynamics results was done by comparing them with flow parameters measured in a 1:5 scale model of the first pass header in the laboratory. Computational fluid dynamics simulations were used to establish hydrodynamic similarity between the 1:5 scale and full scale models of the first pass header. It was found that the erosion–corrosion damage seen at the tubesheet of the first pass header was a consequence of increased levels of turbulence at the tubesheet caused by a rapidly turning flow. A prismatic flow corrections device introduced in the past helped in rectifying the problem at the tubesheet but exaggerated the erosion–corrosion problem at the first pass header shell. A number of alternative flow correction devices were tested using computational fluid dynamics. Axial ribbing in the first pass header and an inlet flow diffuser have shown the best performance and were recommended for implementation. Computational fluid dynamics simulations have revealed a smooth orderly low turbulence flow pattern in the second, third and fourth pass as well as the exit headers where no erosion–corrosion was seen in practice. This study has confirmed that near-wall turbulence intensity, which can be successfully predicted by using computational fluid dynamics, is a good hydrodynamic predictor of erosion–corrosion damage in complex geometries.

© 2006 Published by Elsevier Ltd.

Keywords: Computational fluid dynamics; Erosion–corrosion

1. Introduction

Bauxite refineries frequently utilize what is known as the “Bayer process” in the production of aluminium oxide (alumina) from bauxite ore (King, 1987). Bauxite can typically be found close to the surface of the earth in seams varying from 1 to 10 m in the form of small reddish pebbles. Alumina (aluminium oxide Al_2O_3) is a granular white material which is further processed to obtain aluminium. The Bayer process was discovered by an Austrian chemist Karl Josef Bayer in 1887 and involves (a) dissolving aluminium component of the bauxite ore in a sodium hydroxide solution (caustic soda); (b) removing impurities from the solution; (c) precipitating alumina

trihydrate; (d) calcination to aluminium oxide. Large quantities of caustic soda solution are recycled through a bauxite refinery and the bauxite ore is added at a high temperature, impurities are separated at an intermediate temperature, and alumina is precipitated at the low temperature point in the cycle.

As a part of the Bayer process, the caustic solution is passed through shell-and-tube heat exchangers (HEX) in order to regenerate heat. Regularly the HEX are cleaned and de-scaled by using inhibited mineral acid. The headers of these HEX, which are constructed of mild steel, are regularly inspected for erosion–corrosion damage. Online, this is typically done by using ultrasonic measurements of shell thickness. Occasionally they are taken off-line, opened, inspected visually for damage and if needed repaired. Long term data collection has indicated localized damage to certain sections of the HEX tube sheet and header shells. Based on the pattern of damage it was suspected that this damage could be related to the flow pattern of the fluid within the HEX header.

* Chemical Engineering, Institute for Corrosion and Multiphase Technology, 342 West State Street, Athens, OH 45701, USA. Tel.: +1 740 593 9945; fax: +1 740 593 9949.

E-mail address: nesic@ohio.edu.

Erosion–corrosion is defined as a process in which there is an accelerated loss of metal due to the relative movement of a corrosive fluid over a metal surface (Fontana, 1986). In most cases the protective surface layer on the metal is either eroded or the formation of the layer is altered as a result of flow. In the case of HEX headers, it is speculated that the protective layer formed on the mild steel surfaces in caustic solutions is removed or never forms properly due to fluid flow, which then in turn facilitates base metal loss by the corrosive action. As there was no evidence of solid particles present in the liquid any effect of hydrodynamics on corrosion would have occurred in single phase flow.

To confirm this hypothesis it was decided to use computational fluid dynamics (CFD) to search for the link(s) between the observed pattern of attack seen in practice and the hydrodynamics in the HEX header. CFD nowadays provides an option to look into fluid flow, which is often cheaper than experimentation, can provide detailed results and is suitable for almost any complex geometry. However, computational solutions are based on mathematical models which approximate reality with varying degrees of accuracy. Therefore, solutions obtained by computations need to be validated with experiments whenever possible and interpreted carefully. The fact that large volumes of plausible hydrodynamic results can be rapidly generated with commercial CFD packages can lead to superficiality where meaningful content is obscured by the colourful presentations of the results and good looking imagery. This does not take away from the great potential that CFD has in helping engineers to cope with complex fluid dynamics problems, it just points to a frequent aberration/abuse of the CFD technique.

To gain confidence in the validity of the CFD results, small scale hydrodynamic experiments were conducted at the beginning of this project on a one-fifth scale (1:5) laboratory model of the HEX. For the picture of the 1:5 scale model see Fig. 1. Once confidence in CFD results was established by simulating the flow in the 1:5 scale model, scaling up the hydrodynamic simulation from the model to full scale was a relatively simple and cheap exercise by using CFD, something that would be very costly if not impossible to do empirically. CFD was also used to investigate geometrical modifications that would alter the flow pattern and alleviate the erosion–corrosion problem.

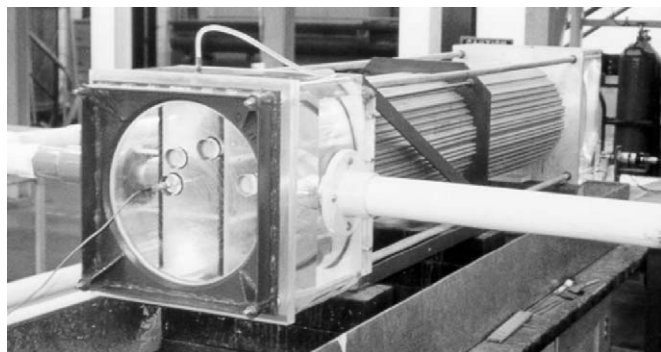


Fig. 1. The 1:5 scale model of the shell-and-tube HEX tested in the laboratory.

2. Experimental background

Lai (1977), Bremhorst and Lai (1979), Lai and Bremhorst (1979), Bremhorst and Flint (1991), empirically examined the flow patterns inside the one-fifth scale model HEX header, the same one as shown in Fig. 1. The main concern at the time was the erosion–corrosion damage occurring at the tube inlets (tubesheet). Consequently, the main hydrodynamic parameter studied was velocity distribution near the tube inlets. Bremhorst and co-workers determined that the cross flow pattern (parallel to the tube sheet) was the main reason for the erosion–corrosion of the tube inlets. Their experiments tested various flow correction devices that would alter the flow pattern so that the bulk of the flow would approach the tube inlets axially. It was from this study that the prismatic flow correction devices were recommended and then installed at the plant. Long term use has proven to have been beneficial and on-balance less damage to the tube inlets has been seen. However, it was suspected that the changed flow pattern may have caused an increase in the damage rate to the shell.

The exact mechanism of erosion–corrosion by which the protective oxide layer is initially removed or its formation inhibited is not yet well understood. Studies conducted in recent years have suggested some possible mechanisms. A relevant study concerning tube inlet damage was published by Elvery (1995) and Elvery and Bremhorst (1997). The main hydrodynamic parameters under consideration were the wall pressure and wall shear stresses present in the tube inlets for varying inlet inclined flow conditions. The results obtained compared well with observed damage in tube inlets and pointed to the importance of the areas near the reattachment point of the recirculation region formed by the inclined flow. The mean wall shear stresses were thought to be too small to mechanically remove the metal's protective layer. This led them to believe that mean wall shear stresses alone were not responsible for removal of the oxide layers, and suggested that another mechanism had to be responsible.

Nešić and Postlethwaite (1990) suggested that near wall turbulent kinetic energy was responsible for the mechanical protective film removal and enhanced mass transfer rates in corrosion of metals. The study carried out for single-phase flows showed that localized, near wall turbulent kinetic energy was responsible for enhanced mass transfer rates. Nešić and Postlethwaite (1990) believed that the intensive near wall turbulence disrupts both the protective oxide layer of the base metal and also the mass transfer boundary layer, which leads to the enhanced corrosion and subsequent failure of metals. Consequently, the studies in the present project focussed on the near wall turbulent kinetic energy, as it was believed that this was one of the most likely factors that could contribute significantly to the observed erosion–corrosion damage.

A recent experimental study was conducted by Coles (2000) as a part of the present project. The purpose of this experimental study was to validate the CFD results for the one-fifth scale model. The experimental results found good agreement with the numerical model, except for some instances

where the hot wire probe vibrations interfered with the velocity measurements.

3. Computational fluid dynamics study

CFD is a numerical technique which relies on solving fundamental equations of fluid motion to get the flow field. The most general set of equations that describe Newtonian fluid flow are the well known Navier–Stokes equations. Due to their complexity (they are three dimensional, transient, nonlinear, partial differential equations) Navier–Stokes equations have not been solved analytically to date. On the other hand numerical procedures have been developed in the past few decades that enable obtaining approximate solutions of Navier–Stokes equations for a wide variety of flow problems. Given the rapid development and availability of faster computers, progressively more complex flow problems can be tackled by the engineers nowadays. Commercial software packages are making this task ever so easier.

Navier–Stokes equations describe equally well both laminar and turbulent flow, however, obtaining solutions for fully turbulent flow fields is still a complex task involving vast quantities of data and long computational times. The technique that is used to achieve this is called direct numerical simulation (DNS) of the Navier–Stokes equations and is practically feasible only for flow at low Reynolds numbers through simple geometries (e.g. flat channel, straight pipe with or without small obstacles). Even then some of the largest supercomputers around need to be utilized to get the solution in a reasonable time-frame. Notwithstanding that, most practical flows are turbulent and a variety of approximate techniques have been developed to simulate highly turbulent flow. Most of them revolve about the idea that for most practical purposes it is sufficient to fully resolve only the main (mean) flow by solving simplified Navier–Stokes equations, while the finer details of turbulence can be approximated from correlations and/or simpler auxiliary equations. The most popular has been the approach where the Navier–Stokes equations are time-averaged to obtain the steady-state Reynolds averaged Navier–Stokes (RANS) equations which are solved in space to obtain the mean flow field. In association with this technique, the turbulence can be approximated in a number of ways and a method which has gained much popularity in the past few decades is the so-called $k-\epsilon$ model combined with the wall-function approach, which was utilized in this study. For more details the reader is directed to many good textbooks on CFD and turbulence modelling, for example Patankar (1980) or Versteeg and Malalasekera (1995) for a basic introduction or Ferziger and Perić (1996) for a more advanced text.

The CFD simulations done in this project were conducted using a widely available commercial CFD package (FLUENT V4.0). The work was done as a sequence of final year thesis projects by honours students at the Mechanical Engineering Department at The University of Queensland. In the initial study Huber (1999) used CFD to investigate qualitatively the flow pattern in the first pass of the shell-and-tube HEX header. He

indicated that there were certain similarities between the fields of predicted near wall kinetic energy of turbulence and the observed erosion–corrosion damage. This work was followed by Rode-Bramanis (2000) who used the same package to simulate the 1:5 scale model of the first pass header with and without the prismatic modifier installed in the field on a large number of units. He found good agreement with the hot-wire measurements by Coles (2000) as mentioned above. In the same year Purchase (2000) conducted a full-scale computational study of both geometries (with and without the prism) and found similar flow patterns as observed in the 1:5 scale model. Following this Varela (2000), Salameh (2001) and Scott (2001) used CFD to look at rectifying the flow pattern in the first pass of the HEX header with an aim to reduce the damage to the shell that was apparently caused by the addition of the prism. Varela (2001) also studied the details of the flow pattern at the inlet to the tubes finding that the high near wall turbulence created by cross flow did indeed correspond to more damage seen in practice. Ainsbury (2001) used CFD to look at flow patterns in the second, third, fourth pass headers, as well as the exiting header where no damage was reported and found that this is related to smooth and orderly low-turbulence flow pattern. A summary of the findings made by this group of talented graduating students is presented below.

4. Results

Before presenting the results it is important to specify some of the more important parameters that were used in the simulations. The outline of the flow geometry which was the primary focus of the CFD simulations, i.e., first pass header is shown in Fig. 2 (without and with the prismatic flow correction device). Note that due to symmetry only the upper half of the header was simulated.

For all CFD simulations the following boundary conditions were used:

- *Inlet*: a convective flux; the inlet velocity was set to 1.5 m/s for the 1:5 scale model and 2.7 m/s for the full scale model; a uniform velocity profile was used with a sufficient entry length to achieve fully developed pipe flow at the entry into the first pass HEX header; turbulence intensity was set at 10% what was acceptable given the sufficient entry length provision.
- *Solid walls*: zero velocity and the standard *wall function* approach which uses semi-empirical formulas to approximate the flow in the boundary layer; typical y^+ values obtained ranged from 30 to 150.
- *Symmetry*: to reduce the size of the computational domain and thus save valuable computational time this boundary condition was used which assumes a zero gradient of all properties across the plane of symmetry.
- *Tube bundle and tubesheet*: were approximated by a porous volume with a much higher permeability in the pipe direction; the real geometry of the tubesheet and the tube bundle was too detailed and complex to include in the present model.

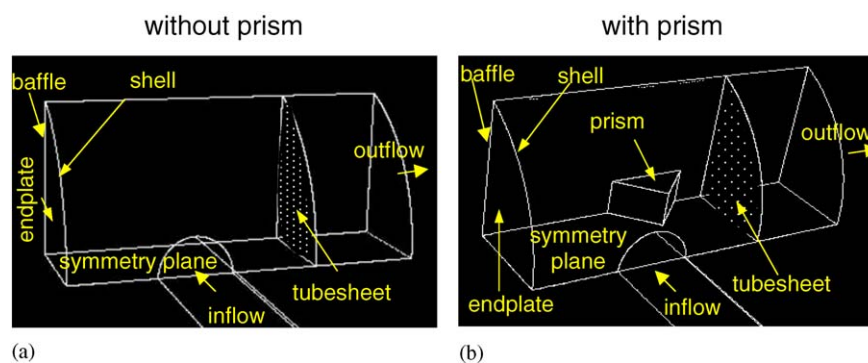


Fig. 2. The side view outline of the upper half of the first pass HEX header simulated by using CFD; (a) without and (b) with prismatic flow correction device.

A second order accurate numerical scheme was used. The convergence criteria needed to be set, which signal when the approximate solution is judged to be sufficiently accurate. For the majority of the runs, the only convergence criteria used were the unscaled residuals of all points in the domain which were required to drop by five orders of magnitude during the simulation, relative to the initial value. Grid independence of the solution was established by repeating the simulations on a sequence of ever so finer non-uniform structured computational grids (thereby increasing the spatial resolution of the calculated answer) until sufficient accuracy was achieved. A final answer was judged to be sufficiently accurate if the changes in the key control parameters from one grid to the next finer one was less than 1%. The total number of tetrahedral control values for a typical simulation varied from 200,000 to 1,500,000.

4.1. Comparison of 1:5 and full scale results for the first pass header

After successfully verifying the CFD simulations for a 1:5 scale model by comparing with the hot-film measurements done in the lab (Coles, 2000; Rode-Bramanis, 2000), it was important to establish hydrodynamic similarity between the 1:5 scale and full scale models. The same inlet pipe Reynolds number was used as the similarity criterion. Simulations were performed for the both flow geometries and indeed it took much longer to get the answer for the full scale model where a 100 times more computational nodes were used. It was gratifying to find out that the flow patterns obtained in the two scale models was very similar as indicated in Fig. 3 where characteristic pathlines are shown. Many more qualitative hydrodynamic parameters were obtained and compared for the two geometries with the same success; however their presentation exceeds the scope of this paper (see for example Purchase, 2000).

It can be seen on all the plots in Fig. 3 that upon entering the first pass header the fluid goes into a large swirl that approaches the tubesheet at a high angle of incidence only to rapidly turn there and enter the tubes. A portion of the inflow initially turns away from the tubesheet and moves towards the front plate, turns around there and spirals rapidly

towards the tubesheet. These simulations confirmed the experimental findings of Bremhorst and co-workers (1977–1991) who indicated significant “cross flow” at the tube sheet. From Fig. 3 it appears that the prismatic flow correction device that was suggested as a remedy by Bremhorst and co-workers (1977–1991) did not achieve much in terms of rectifying the flow pattern, a fact not completely born out by a subsequent more in-depth analysis of the key flow parameters as discussed below.

4.2. Flow pattern vs. erosion–corrosion damage for the first pass header

In long term (a decade long) observations on the real HEX, a consistent pattern of damage was observed at the tubesheet. The inlets to certain groups of tubes were affected more than others and a typical damage pattern for the tubesheet in the full scale first pass header of a shell-and-tube HEX is shown in Fig. 4. This particular damage pattern is what signalled that the attack might be flow related and prompted Bremhorst and co-workers (1977–1991) to study the flow pattern and propose the prism as a flow correction device. The CFD simulations done for a full scale first pass HEX header without and with the prismatic flow correction device have revealed that the introduction of the prism did change the angle of incidence of the fluid as it approached the tubesheet (see Fig. 5) as Bremhorst and co-workers (1977–1991) has claimed. Even if this is not obvious in the qualitative plots of the pathlines shown in Fig. 3, upon closer inspection of the data it was found that the prism deflected more of the incoming fluid away from the tubesheet and toward the endplate what gave it a longer path and a better chance to align the approach to the tubesheet. As a consequence less twisting and turning of the fluid occurred at the tubesheet resulting in lower degree of turbulence as shown in Fig. 6. Note that the same scale for the kinetic energy of turbulence was used in all the plots in this paper so that they can be qualitatively compared (low value being 0 and the high value being $0.134 \text{ m}^2/\text{s}^2$). Given the variability of the damage pattern from one to another HEX, there is rather good match of the predicted level of near-wall turbulence intensity shown in Fig. 6a and the observed pattern of damage for one of the

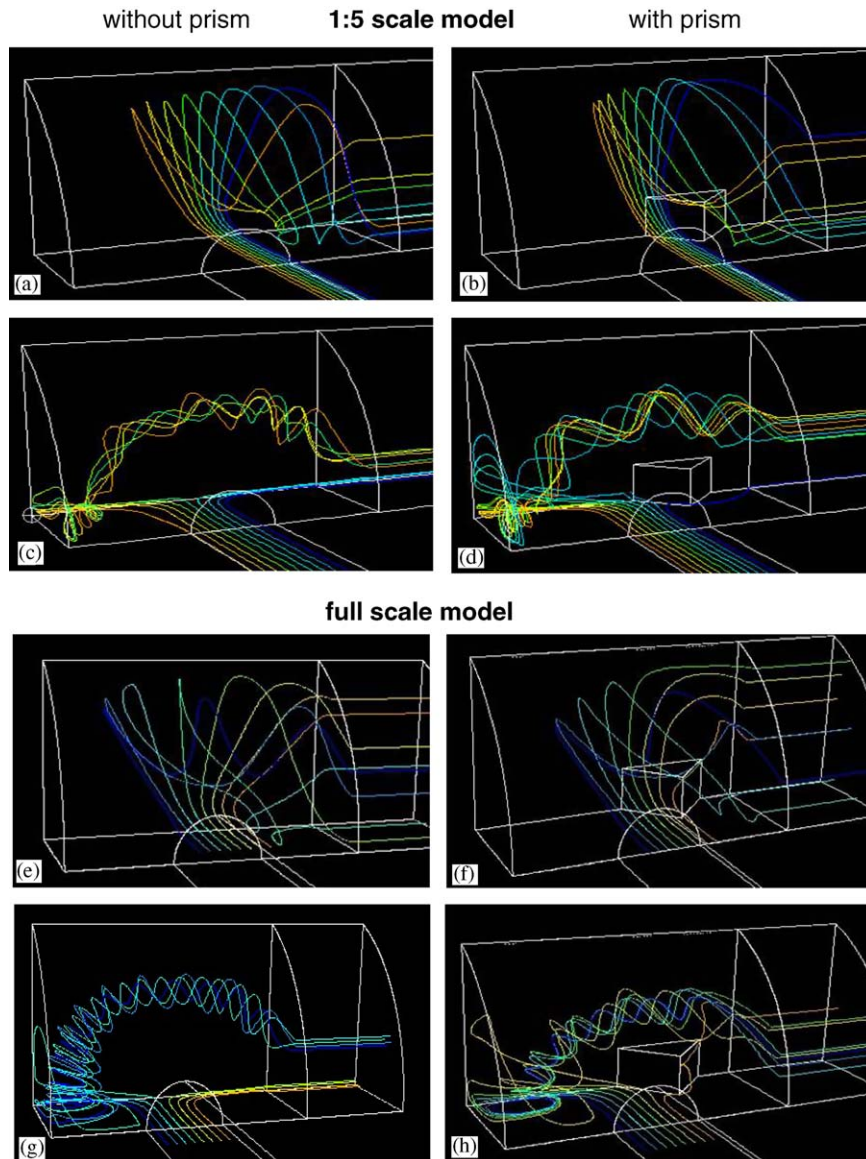


Fig. 3. Comparison of CFD simulations of flow in a first pass HEX header for a 1:5 scale model (a–d) and a full scale model (e–h) both without (left) and with (right) the prismatic flow correction device. A side view of a sample of representative pathlines is shown. Colours denote different starting point for the pathlines.

HEX seen in Fig. 4. This has confirmed the hypothesis that near-wall turbulence intensity could be a good hydrodynamic predictor of expected erosion–corrosion damage. It still cannot be known what the exact mechanism is however there are a few possibilities:

- increased near-wall turbulence promotes mass transfer i.e., the transport of the corrosive species from the bulk fluid to the metal surface what increases corrosion as well as transport of corrosion products away from the metal surface, thereby preventing them to form a protective scale/film which would reduce corrosion;
- increased near-wall turbulence leads to enhanced levels of fluctuating hydrodynamic stresses (both pressure and shear), what can lead to mechanical damage of an existing pro-

TECTIVE surface layer or can prevent it from forming in the same way.

However, there were suspicions that the introduction of the flow correction prism, more than two decades ago, has on average increased the rate of damage to the HEX shells. This was suggested by long term ultrasonic shell thickness measurements. Even if there was some variability in the pattern of observed damage, there appeared to be a critical area where the damage was more pronounced (see Fig. 7) The critical area stretched in the axial direction closer to the baffle. By observing the flow pattern in Fig. 3 it is immediately apparent that this could be caused by the large vortex that makes its way from the endplate towards the tubesheet. To confirm this, a plot of near-wall turbulent kinetic energy is shown in

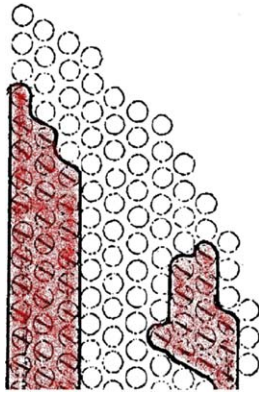


Fig. 4. A typical pattern of erosion–corrosion damage (shaded area) observed at the tubesheet of a first pass HEX header without a prismatic correction device, used in a bauxite refinery. For a matching image of the angle of incidence see Fig. 5 and for the turbulent kinetic energy see Fig. 6.

Fig. 8 for the cases without and with the prismatic flow correction device. Clearly there is an area of intense turbulence close to the header shell that arises from the above-mentioned vortex. The presence of the prismatic flow correction device has not changed this situation; however it has increased the magnitude of the turbulence near the shell by strengthening the vortex. Therefore, the perception that the prism has solved one problem (at the tubesheet) but has created another (at the shell) was supported by these results, however other factors such as metallurgy, process parameters, etc. would need to be looked at for a more complete explanation.

4.3. Alternative flow correction devices for the first pass header

Once the link between the observed pattern of damage and hydrodynamic parameters was established, CFD was used to

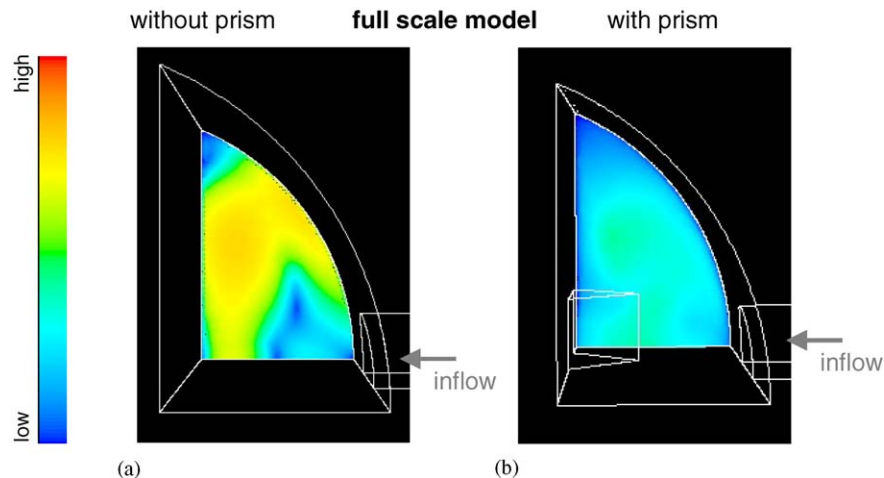


Fig. 5. Frontal view of the contour plots of the angle of incidence at the tubesheet of a full scale first pass HEX header without (left) and with (right) the prismatic flow correction device. Blue denotes small angles i.e., near-axial entry of the fluid into the tubes while yellow/orange denotes large angles i.e., strong cross flow and sharp turning of the fluid entering the tubes. For a matching image of turbulent kinetic energy see Fig. 6 and for the pattern of erosion–corrosion damage see Fig. 4.

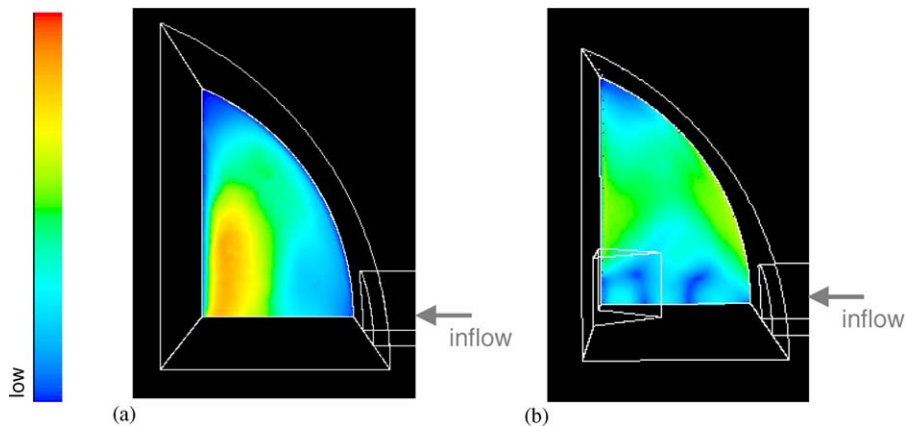


Fig. 6. Frontal view of the contour plots of the turbulent kinetic energy at the tubesheet of a full scale first pass HEX header without (left) and with (right) the prismatic flow correction device. Blue denotes low turbulence while orange denotes high turbulence of the fluid entering the tubes. For a matching image of the angle of incidence see Fig. 5 and for the pattern of erosion–corrosion damage see Fig. 4.

explore alternative flow correction devices that would reduce the levels of near-wall turbulence in the header. The successful design had to solve the perceived flow related erosion–corrosion problem but also had to be simple and cheap to install and maintain. In this spirit, the solutions which were known to be beneficial from a hydrodynamic point of view but were unsuitable for practice were discarded immediately. Examples are various kinds of meshes and other flow straighteners installed close to the tubesheet which would be very difficult to maintain. A small sample of alternatives which were examined by using CFD is presented below.

4.3.1. Deflectors

As it became clear that the prismatic flow correction device was at least partially successful in reducing the problem by

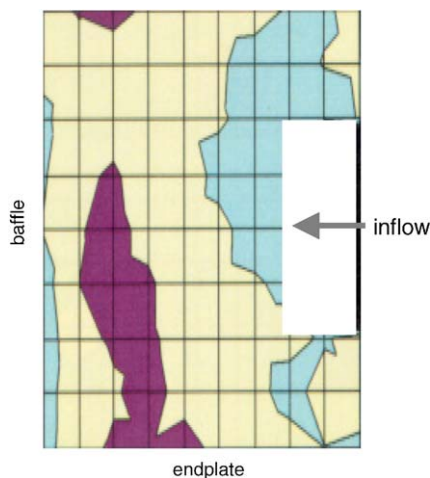


Fig. 7. A top view of a typical pattern of erosion–corrosion damage recorded by ultrasonic thickness measurements at the shell of a first pass HEX header with a prismatic correction device, used in a bauxite refinery. The darker colour indicates more severe damage. For a matching image of the turbulent kinetic energy see Fig. 8.

redirecting the incoming stream of fluid towards the endplate, other flow deflecting devices were examined. Scott (2001) simulated a large number of alternatives. A backward facing plate deflector attached to the inlet which redirected the incoming flow towards the endplate and away from the tubesheet is presented first. The predicted pathlines and the turbulence levels at the tubesheet and the shell are shown in Fig. 9. Clearly a different, yet still chaotic, flow pattern was revealed within the header with a beneficial effect on the HEX shell where the level of turbulence was reduced. However, high levels of turbulence are predicted at the first pass HEX tubesheet and therefore this solution was discarded.

A forward facing plate deflector attached to the inlet which directed the incoming flow towards the tubesheet is presented next. The predicted pathlines and the turbulence levels at the tubesheet and the shell are shown in Fig. 10. The pathlines show that while some of the flow did manage to “squeeze” through directly into the tubes (see Fig. 10a), a large portion of the flow did swerve backwards away from the tubesheet (see Fig. 10b). The end result was unacceptable as extremely high values of near-wall turbulence were predicted across the tubesheet.

4.3.2. Fins

Recall that in the original design of the first pass HEX header the main erosion–corrosion problem arose from high levels of turbulence at the tubesheet (see Fig. 6). This was corrected by the prism, which then created a new problem on the shell by intensifying the vortex that spiralled from the endplate toward the tubesheet (see Fig. 8). As a possible remedy it was thus proposed to try and break-up this vortex by introducing fins into the header as shown in Fig. 11 (Salameh, 2001). The investigation consisted of four models comprised of:

- A single fin running axially along the header.
- A single fin running axially along the header with lesser breadth.

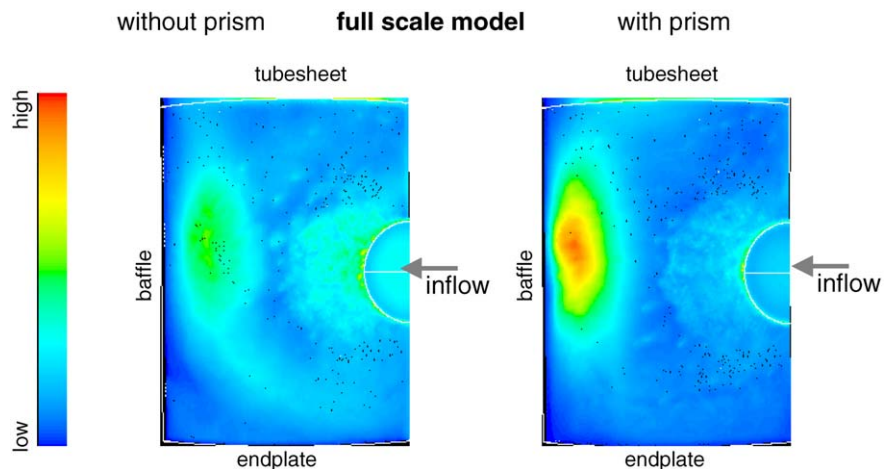


Fig. 8. A top view of the contour plots of the turbulent kinetic energy at the shell of a full scale first pass HEX header without (left) and with (right) the prismatic flow correction device. Blue denotes low near-wall turbulence levels while orange/red denotes high turbulence of the fluid. For a matching image of a typical erosion–corrosion damage pattern see Fig. 7.

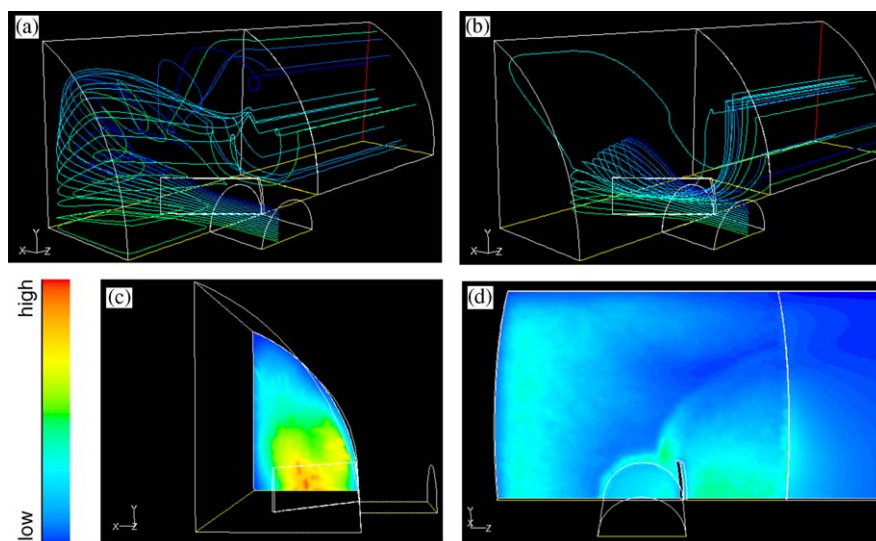


Fig. 9. (a) and (b) Side view of a sample of representative pathlines in a full scale first pass HEX header with a backward-facing inlet flow deflector, with colours denoting different starting point for the pathlines; (c) front view of the contour plots of the turbulent kinetic energy at the tubesheet; (d) side view of the contour plots of the turbulent kinetic energy at the shell. Blue denotes low near-wall turbulence while orange/red denotes high turbulence of the fluid.

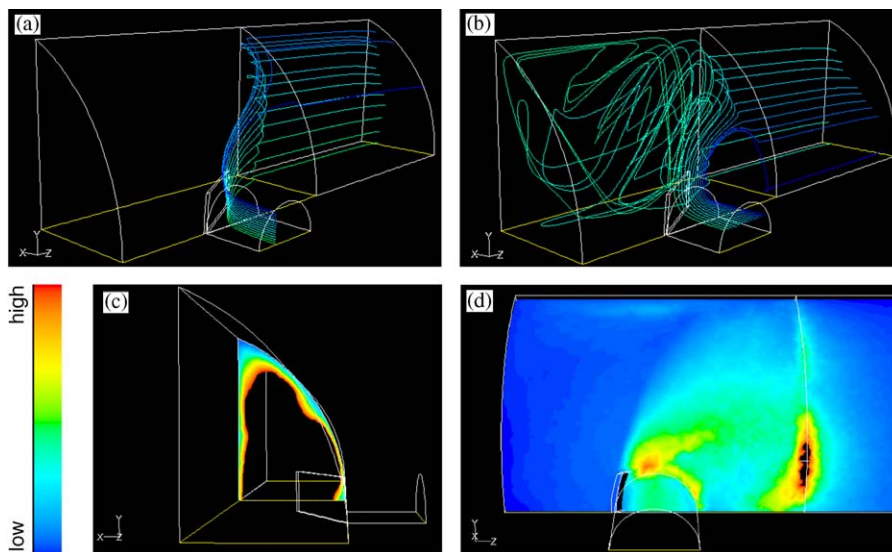


Fig. 10. (a) and (b) Side view of a sample of representative pathlines in a full scale first pass HEX header with a forward-facing inlet flow deflector; colours denoting different starting point for the pathlines; (c) front view of the contour plots of the turbulent kinetic energy at the tubesheet; (d) side view of the contour plots of the turbulent kinetic energy at the shell; blue denotes low levels of near-wall turbulence, orange/red denotes high and black denotes very high values which are off the scale used on all the plots.

- Three fins running axially along the header.
- Three fins running axially along the header with the prism installed.

The four geometries were modelled in succession, such that gradual improvements on the flow parameters within the HEX header were achieved. The first two geometries listed, contributed to the reducing of the turbulent kinetic energy on the header shell but also resulted in the increase in levels of local turbulence in the region of the baffle, which was a

result of an intense new vortex forming in the header. The third model showed success in reducing high levels of turbulence on the header shell by the use of the three fins placed on the shell. The tube sheet however, still displayed problems with respect to the turbulent kinetic energy and impingement angle levels. The final simulation alleviated this problem by reintroducing the prismatic flow corrector. With this solution some vorticity in the header was still present as evident by the pathlines (see Fig. 11a), however, the level of turbulence both at the tubesheet (see Fig. 11c) and particularly at the shell

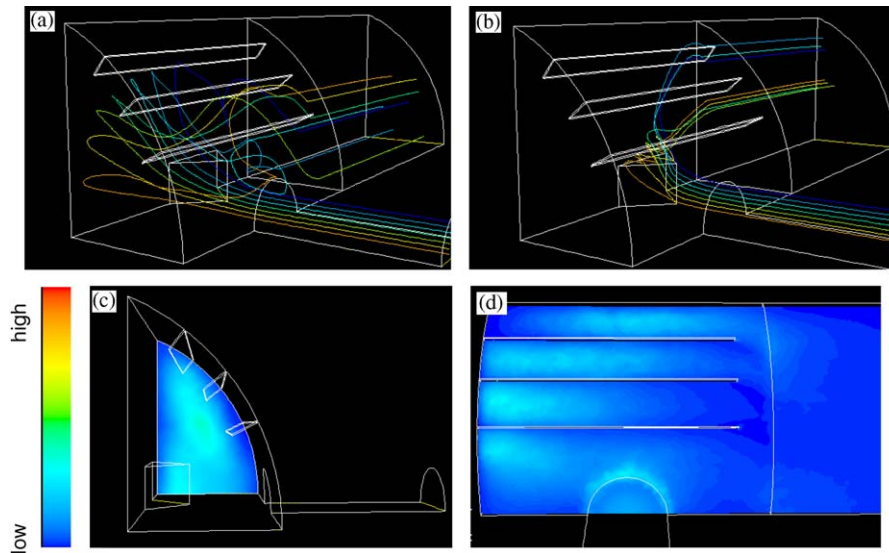


Fig. 11. (a) and (b) Side view of a sample of representative pathlines in a full scale first pass HEX header with a three ribs and a prismatic flow correction device; colours denoting different starting point for the pathlines; (c) front view of the contour plots of the turbulent kinetic energy at the tubesheet; (d) side view of the contour plots of the turbulent kinetic energy at the shell; blue denotes low levels of near-wall turbulence.

(see Fig. 11d) was significantly reduced (almost by an order of magnitude). Due to this beneficial effect and the simplicity of introducing this flow correction device it was considered for implementation.

4.3.3. Diffuser

Stepping back and rethinking the original design of the first pass HEX header it became clear that the whole problem arose from the way flow enters the header in the form of a high velocity jet. The jet swirls around the header, eventually slows down and leaves via the tubes, causing erosion–corrosion problems in the meanwhile. Therefore, as a possible remedy it was proposed to slow the flow down before it enters the header by introducing a bell diffuser (Varela, 2000). A diffuser with a 50% area ratio was decided upon as it appeared effective and practically feasible (see Fig. 12). In this design, no separation of the flow in the diffuser was occurring and the flow pattern inside the header appeared qualitatively unchanged as indicated by the pathlines shown in Fig. 12a–d. Some of the flow went straight towards the tubesheet while a significant portion initially moved away from the tubesheet towards the endplate turned there and finally spiralled forward. The same occurred irrespective of the prism, the only difference being that with the prism a larger portion of the flow was redirected backward towards the endplate, just like in the original design shown in Fig. 3. However, there is one key difference when comparing the new and the old design: the magnitude of all the critical hydrodynamic parameters in the header was much lower with the new design as the inlet jet velocity was cut down in half. This is evident by looking at the levels of turbulence at the tubesheet (Fig. 12e–f) and at the shell (Fig. 12g–h), which were reduced one order of magnitude. The diffuser appeared to be the best practical solution as it would rectified the flow pattern

to alleviate the erosion–corrosion problem (irrespective of the prism) and it would be easy to install without much alterations to the original header. In addition it seemed very unlikely that any problems would be created by installing the diffuser. This design was recommended for implementation and long term testing in the bauxite refinery.

4.4. Other headers

In practice damage was only experienced within the first pass HEX header. The four other headers suffered extremely little or no erosion–corrosion in service. At the first glance this appears to be peculiar as all the headers are made from the same mild steel and experience virtually the same operating conditions. The only exceptions are:

- Small variations in the temperature of the fluid which increases as the fluid flows from one header to another.
- The flow pattern in the various passes is significantly different.

From a theoretical point of view the small increase in temperature cannot explain the large differences in the observed magnitude of erosion–corrosion damage. In addition, the same fluid that does little or no damage to the second, third, fourth and exit headers of one HEX flows to the next HEX in line and the damage occurs again in the first pass only even if the temperature there is even higher. This suggests that a factor other than temperature must be responsible for the pattern of damage. Given the rationale laid out above, where disturbed flow and near-wall turbulence were linked to erosion–corrosion damage, one would expect to see very smooth flow with little or no turbulence in the second, third,

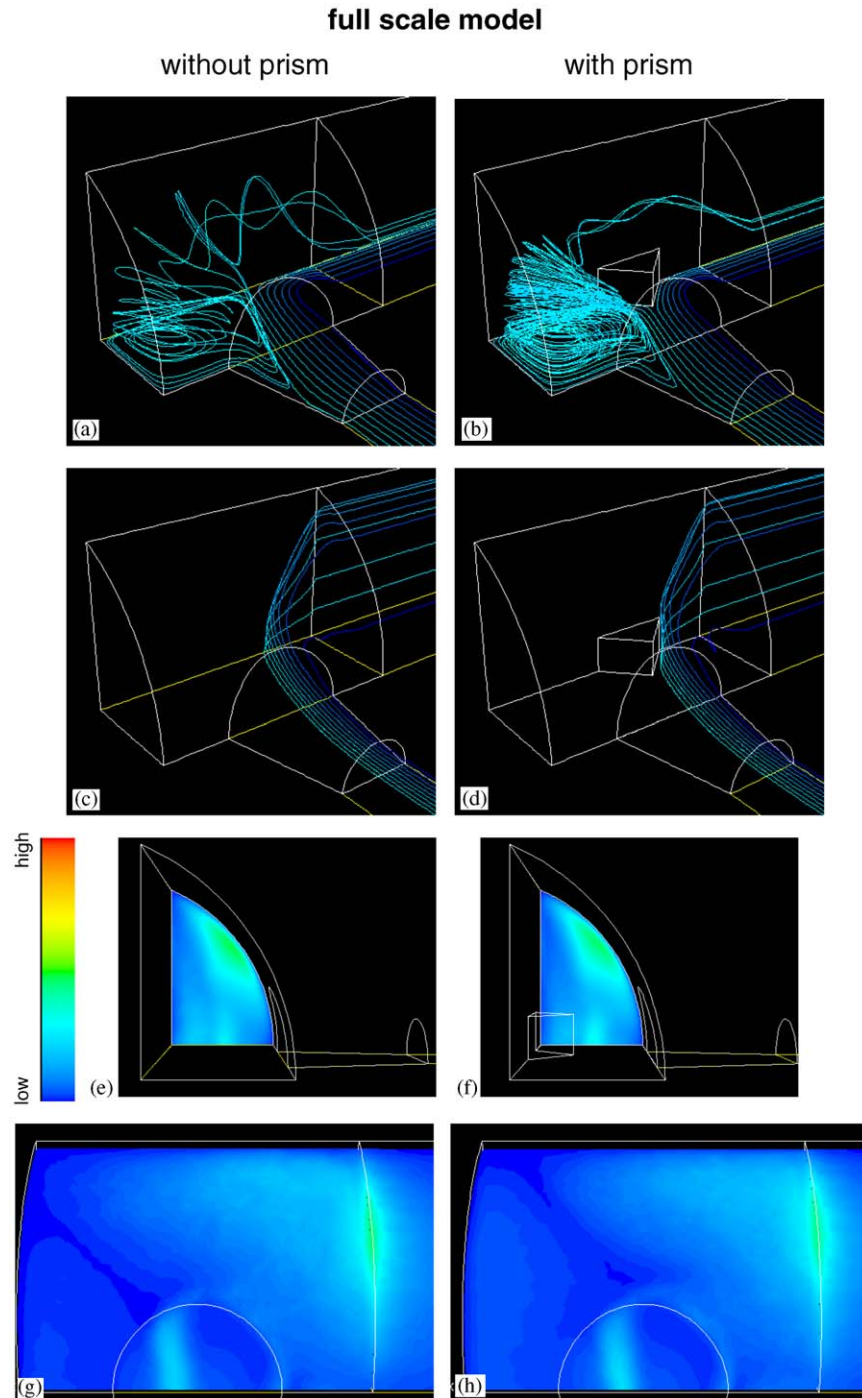


Fig. 12. (a–d) Side view of a sample of representative pathlines in a full scale first pass HEX header including a diffuser without (left) and with (right) prismatic flow correction device; colours denoting different starting point for the pathlines; (e–f) front view of the contour plots of the turbulent kinetic energy at the tubesheet; (g–h) side view of the contour plots of the turbulent kinetic energy at the shell; blue denotes low and green moderately high levels of near-wall turbulence.

fourth and exit headers. This would explain the lack of damage in these headers and the sharp contrast with the first pass header. An investigation was undertaken by Ainsbury (2001) and indeed he discovered smooth undisturbed flow in all the remaining headers. As an illustration orderly smooth flow and

low levels of turbulence at the tubesheet can be seen in the second pass header (see Fig. 13) as well as the third pass header (see Fig. 14). Similar results were observed for the fourth pass header and the exit header. This finding confirmed the operating assumption about the near-wall turbulence intensity being

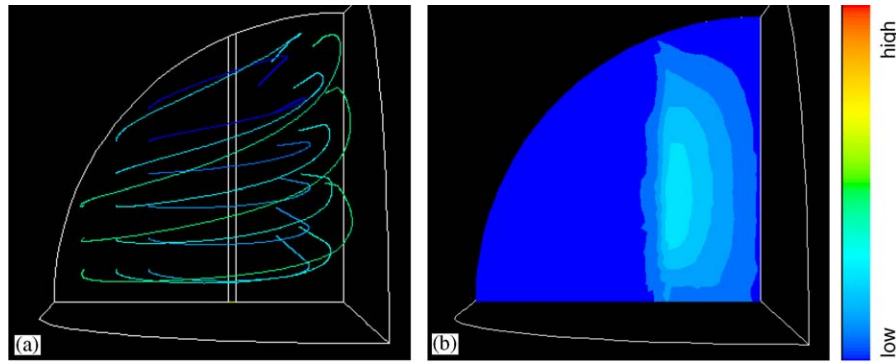


Fig. 13. (a) Back view of a sample of representative pathlines in a full scale second pass HEX header including; colours denoting different starting point for the pathlines; (b) back view of the contour plots of the turbulent kinetic energy at the tubesheet; blue denotes low levels of near-wall turbulence.

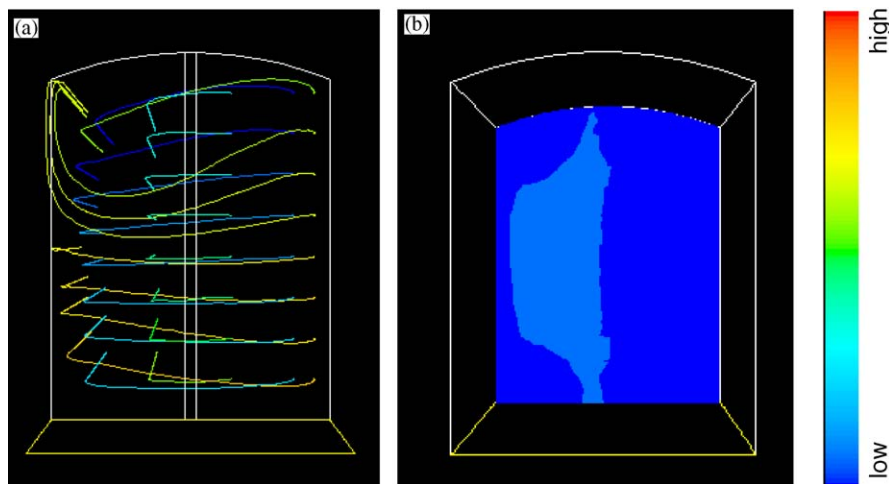


Fig. 14. (a) Front view of a sample of representative pathlines in a full scale third pass HEX header including; colours denoting different starting point for the pathlines; (b) front view of the contour plots of the turbulent kinetic energy at the tubesheet; blue denotes low levels of near-wall turbulence.

a good hydrodynamic predictor of erosion–corrosion of mild steel.

5. Conclusions

- CFD was used to search for the link(s) between the observed pattern of attack seen in a bauxite refinery heat exchanger first pass header and the hydrodynamics inside the header.
- Validation of the CFD results was done by comparing them with flow parameters measured in a 1:5 scale model of the first pass header in the laboratory.
- CFD simulations were used to establish hydrodynamic similarity between the 1:5 scale and full scale models of the first pass header.
- It was found that the erosion–corrosion damage seen at the tubesheet of the first pass header was a consequence of increased levels of turbulence at the tubesheet caused by a rapidly turning flow. A prismatic flow corrections device introduced in the past helped in rectifying the problem at the

tubesheet but exaggerated a erosion–corrosion problem at the first pass header shell.

- A number of alternative flow correction devices were tested using CFD. Axial ribbing in the first pass header and an inlet flow diffuser have shown the best performance and were recommended for implementation.
- CFD simulations have revealed a smooth orderly low turbulence flow pattern in the second, third and fourth pass as well as the exit headers where no erosion–corrosion was seen in practice.
- This study has confirmed that near-wall turbulence intensity, which can be successfully predicted by using CFD, is a good hydrodynamic predictor of erosion–corrosion damage in complex geometries.

Acknowledgments

The author was fortunate to have worked with a generation of talented graduating students at The University of Queensland

Mechanical Engineering Department who were all (one way or another) part of this effort. They are, in no particular order: Phillip M. Huber, Christopher Hutchins-Sach, Shane Coles, Ann M. Purchase, Steven Rode-Bramanis, Tarek Salameh, Michael P. Scott, Carlos A. Varela and Matthew P. Ainsbury.

References

- Ainsbury, M.P., 2001. Computational investigation of erosion–corrosion in the 2nd, 3rd and 4th pass header of a shell and tube heat exchanger. Undergraduate Thesis, University of Queensland, Brisbane.
- Bremhorst, K., Flint, P.J., 1991. *Wear* 145, 123–135.
- Bremhorst, K., Lai, J.C.S., 1979. *Wear* 54, 87–100.
- Coles, S., 2000. Hydrodynamic investigation of erosion–corrosion in a shell and tube heat exchanger header. Undergraduate Thesis, University of Queensland, Brisbane.
- Elvery, D.G., 1995. Erosion–corrosion in tube inlets as a consequence of inclined flow into heat exchangers. Ph.D. Thesis, UQ, Brisbane.
- Elvery, D.G., Bremhorst, K., 1997. *Journal of Fluids Engineering* 103, 948–953.
- Ferziger, J.H., Perić, M., 1996. *Computational Methods for Fluid Dynamics*. Springer, Berlin.
- Fontana, M.G., 1986. *Corrosion Engineering*. third ed. McGraw-Hill Book Company, USA.
- Huber, P.M., 1999. CFD study of erosion–corrosion in a shell and tube heat exchanger header. Undergraduate Thesis, University of Queensland, Brisbane.
- King, F., 1987. *Aluminium and its Alloys*. Ellis Horwood Limited, Chichester, UK, pp. 39–44.
- Lai, J.C.S., 1977. Hydrodynamic aspects of erosion–corrosion of tube inlets of shell and tube heat exchangers. Masters Thesis, UQ, Brisbane.
- Lai, J.C.S., Bremhorst, K., 1979. *Wear* 54, 101–112.
- Nešić, S., Postlethwaite, J., 1990. *Corrosion* 46 (11), 874–880.
- Patankar, S.V., 1980. *Numerical Heat Transfer and Fluid Flow*. McGraw-Hill Book Company, New York.
- Purchase, A., 2000. CFD investigation of erosion–corrosion in the first pass of a shell and tube heat exchanger. Undergraduate Thesis, University of Queensland, Brisbane.
- Rode-Bramanis, S., 2000. Investigation into the hydrodynamic parameters contributing to erosion–corrosion in a shell and tube heat exchanger header. Undergraduate Thesis, University of Queensland, Brisbane.
- Salameh, T., 2001. Computational fluid dynamics investigation of erosion–corrosion in a heat exchanger header. Undergraduate Thesis, University of Queensland, Brisbane.
- Scott, A., 2001. Computational fluid dynamics investigation of erosion–corrosion in a heat exchanger header. Undergraduate Thesis, University of Queensland, Brisbane.
- Varela, C., 2000. Report of UQ research on erosion–corrosion damage in a shell and tube heat exchanger. Vacation Work Report, University of Queensland, Brisbane.
- Varela, C., 2001. Computational fluid dynamics study of erosion–corrosion on shell-and-tube exchanger tube inlets. Undergraduate Thesis, University of Queensland, Brisbane.
- Versteeg, H.K., Malalasekera, W., 1995. *An Introduction to Computational Fluid Dynamics*. Longman, White Plains, NY.

Further Reading

- Hutchins-Sach, C., 1999. Computational investigation of erosion–corrosion in a tube and shell heat exchanger header. Undergraduate Thesis, University of Queensland, Brisbane.